Clays and Clay Minerals, Vol. 59, No. 6, 560–567, 2011.

POWDER X-RAY DIFFRACTION STUDY OF THE HYDRATION AND LEACHING BEHAVIOR OF NONTRONITE

NICOLA V. Y. SCARLETT[1,*], MARK RAVEN[2], AND IAN MADSEN[1]

[1] CSIRO Process Science and Engineering, Box 312, Clayton South, Victoria, 3169, Australia
[2] CSIRO Land & Water, Waite Rd, Urrbrae, South Australia, 5064, Australia

Abstract—Nontronite is a significant component of commercially important nickel laterite ores. Its behavior during high-pressure acid leaching of such ores may have an impact upon the efficiency of the process. The present study was conducted in order to further investigate the response of this material during high-pressure acid leaching. *In situ* synchrotron powder X-ray diffraction data were collected from a number of nontronite samples during hydration and leaching reactions at ambient and elevated temperatures. The present study followed previous high-pressure acid-leaching studies of nontronite where unexpected contraction and expansion behavior of the clay was observed by means of *in situ* X-ray diffraction. In the earlier studies the data sets only extended to ~20 Å so that when the nontronite expanded to greater than 19.5 Å (hydrated) the main 001 peak was only partially visible in the observed *d*-spacing range. The aim of the current work was to collect similar *in situ* diffraction data over a greater *d*-spacing range to observe more fully the movement of the main 001 reflection in order to better understand the changes taking place. This work was undertaken at the powder diffraction beamline of the Australian Synchrotron which was configured such that an upper *d*-spacing limit of ~34.5 Å could be achieved. Suggestions arising out of the previous work were confirmed along with additional information from testing of samples from the Source Clays Repository of The Clay Minerals Society. These results also show contradictory behavior of clays with the layer charge distributed over tetrahedral and octahedral sheets.

Key Words—High-pressure Acid Leaching, Nontronite, Powder XRD, Time-resolved XRD, Synchrotron.

INTRODUCTION

Nontronite is a significant component of commercially important Ni-laterite ores. Ni-laterites are low-grade Ni-bearing ores but represent ~70% of the world's resources of this valuable metal (Dalvi *et al.*, 2004). High-pressure acid leaching (HPAL) in sulfuric acid at elevated temperatures and hydrothermal pressure is used to extract the nickel from the ores commercially. The cooled, Ni-rich solution is subsequently processed to recover the metal. *In situ* X-ray diffraction (XRD) experimentation has been developed (Madsen *et al.*, 2005; Norby *et al.*, 1998) to study dynamically the phase changes taking place during the leaching process.

The aim of the present work was to examine in more detail the swelling and contraction behavior of nontronite during hydration and acid leaching. The 001 reflection of this mineral is very sensitive to the interlayer spacing of the clay and as such is indicative of the hydration state or effects of acid attack on the structure. The present work stems from previous studies into the HPAL of nontronite where the experimental set-up was such that the full range of movement of this reflection was not seen (Scarlett *et al.*, 2008). The current study was undertaken at the new powder diffraction beamline at the Australian Synchrotron and great care was taken to achieve the lowest possible diffraction angle. Data collection in the previous experiments had only extended to a *d* spacing of ~20 Å; in the present study it started at ~34.5 Å.

The previous high-pressure acid-leaching work used a nontronite (designated Nont2g) from the arid region of Bulong in Western Australia, and the same material was examined again here. This ore and its preparation were described previously (Scarlett *et al.*, 2008; Whittington *et al.*, 2003). The present study also considers two additional nontronites (NAu-1 and NAu-2) from the Uley Graphite mine near Port Lincoln, South Australia. These were described by Keeling *et al.*, (2000) and sufficient bulk samples of both these nontronites were collected to supplement reference nontronite from the Source Clays Repository of The Clay Minerals Society.

EXPERIMENTAL

Sample preparation and environment

The 710 μm fractions of the three nontronites described above were micronized (McCrone micronizing mill, McCrone Research Associates, London) for 5 min g^{-1} (total of 3 g of material in the mill) in ethanol. These ground samples were then spiked with diamond powder (Polishing powder from Proscitech, Australia) to serve as an internal standard at ~20 wt.%.

* E-mail address of corresponding author:
Nicola.scarlett@csiro.au
DOI: 10.1346/CCMN.2011.0590602

The diamond was added in order to monitor beam intensity and to provide a reference point with which to assess the significance of peak movements. Acid solutions were made by mixing concentrated sulfuric acid with water. The 'high acid' solution contained 32.7 wt.% sulfuric acid (0.66 wt.% or 7.7 M H^+), while the 'low acid' solution contained 19.4 wt.% sulfuric acid (0.39 wt.% or 4.3 M H^+). Samples were presented to the beam in one of two ways. The first was a liquid injection method where ~3 mm of dry sample was mounted in the tip of a 1.0 mm quartz glass capillary. About 10 mm of solution was then injected into the capillary leaving an air gap of ~1 mm between it and the dry sample. When ready, the capillary was pressurized using high-purity nitrogen, thus forcing the solution into the sample (Figure 1). The second method of presentation was the same as that described by Scarlett *et al.* (2008) where a slurry of ore and solution was prepared in known concentration and injected into the capillary reaction vessel. A static pressure was then applied using high-purity nitrogen in order to achieve the required temperature without boiling the solution. The pressure applied was slightly in excess of the hydrothermal pressure of water at the selected temperature.

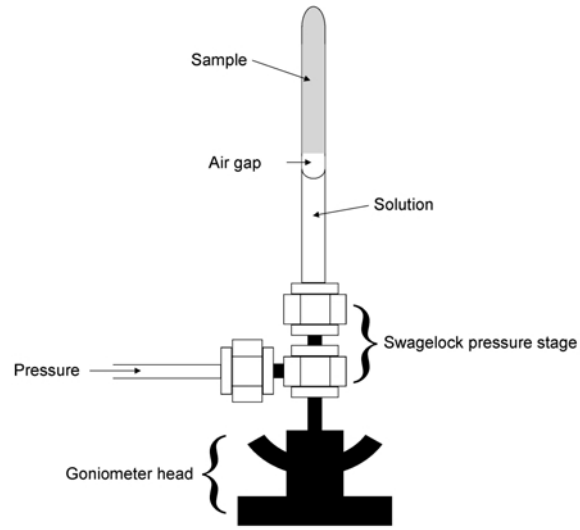

Figure 1. Capillary sample stage for liquid injection experiment showing a sample at end of capillary with an air gap to solution. The capillary is held in the Swagelock pressure stage which is mounted on a goniometer head and allows its alignment in the diffractometer (after Norby, 1998).

Characterization of starting materials

The three nontronites studied here were described previously and structural formulae for NAu-1 and NAu-2 determined (see the Introduction and Table 1). Powder XRD indicated the presence of a small amount of albite (~4 wt.%) in NAu-2 and small amounts (2−4 wt.%) of quartz, clinochlore, and magnesiochromite in Nont2G.

Synchrotron data collection

Synchrotron diffraction data were collected at the Powder Diffraction beamline (10-BM1) at the Australian Synchrotron (AS). The data presented in this study were collected at a wavelength of 1.24 Å. The detector at the synchrotron is the position-sensitive Mythen detector (Schmitt *et al.*, 2003) covering 80º2θ with an inherent resolution of 0.004º2θ. This detector has a series of modules, each covering 5º, with a 0.2º2θ gap between each module.

For each nontronite sample, an experiment was carried out in which one of three solutions (water, low acid, or high acid) was injected into dry powder (liquid-injection method) while diffraction data were collected continuously. The method was used to determine the initial effect of wetting or acid attack on the material. In subsequent experiments, slurries of each combination of nontronite and solution were prepared, injected into capillaries (slurry method), and heated while continuous data collection took place. This was to determine the effect of hydrothermal heating on the reactions. Initial experiments were conducted using a 10 s data collection time with two detector positions ~0.5º2θ apart. The collection of data in this manner allowed the merging of the data and the effective eradication of gaps in the data at the intersection of the detector modules. However, the overall time taken per data set (2×10 s data collection + 2-3 s moving/settling time for detector) was deemed to be too slow to observe the commencement of reaction. Hence the data-collection strategy was modified to a data-collection time of 2 s per data set in a single detector position. In this case, the detector was positioned to ensure that the full range of angular movement of the nontronite peak could be observed within a single detector module.

Table 1. Structural formulae of the two standard nontronites considered in this work. Note that the formulae of NAu-1 and NAu-2 are as determined by Gates *et al.*, (2002) and that Ca and Mg were identified from XRF and EDX (Keeling *et al.*, 2000). Ca^{2+} was assumed to be the dominant exchangeable cation in untreated samples of NAu-1 and NAu-2.

Sample	Interlayer	Tetrahedral	Octahedral	Balance
NAu-1	$M^+_{1.03}$ $(Ca_{0.52})$	$(Si_{6.98}Al_{0.95}Fe_{0.07})$	$(Fe_{3.61}Al_{0.36}Mg_{0.04})$	$O_{20}(OH)_4.nH_2O$
NAu-2	$M^+_{0.71}$ $(Ca_{0.34})$	$(Si_{7.55}Al_{0.16}Fe_{0.29})$	$(Fe_{3.54}Al_{0.34}Mg_{0.05})$	$O_{20}(OH)_4.nH_2O$

https://doi.org/10.1346/CCMN.2011.0590602 Published online by Cambridge University Press

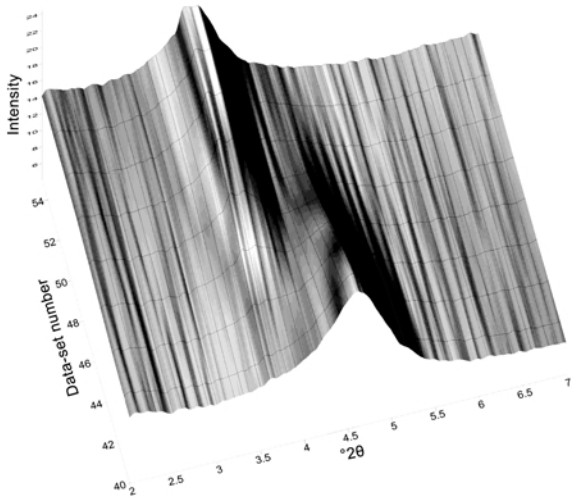

Figure 2. Accumulated synchrotron XRD patterns from the hydration of NAu-1 at room temperature. The data are represented as a three-dimensional plot with diffraction angle (°2θ) along the *x* axis, data-set number along the *y* axis, and intensity along the *z* axis. The 001 reflection of nontronite can be seen to move to a lower diffraction angle (greater *d* spacing) with hydration.

Experiments were also conducted in which the two standard nontronites (NAu-1 and NAu-2) were heated to 300ºC to observe their dehydration behavior. The samples were then cooled and the ends of the capillaries broken and inserted into water-filled capillaries to allow the rehydration of the ore. This had to be done manually so the first moment of rehydration was not observed by diffraction.

Data analysis

The data from each experiment were plotted and assessed qualitatively (Figure 2). The individual diffraction patterns were then analyzed using *TOPAS* (Bruker AXS, 1999) software for peak fitting. The data were modelled with pseudo-Voigt or split pseudo-Voigt (if required) peaks corresponding to the diffraction peaks observed (Figure 3). The refined peak intensities were normalized to the intensity of the diamond internal standard. The data sets were processed as batches and the resultant output of peak positions examined graphically.

RESULTS AND DISCUSSION

Hydration and leaching

The movement of the *d* spacing of the 001 reflection for all combinations of sample and solution was measured and plotted as a function of reaction time (Figures 4–6). In each sample, hydration produced a reduction in intensity of the original 001 reflection with the coincidental growth of a lower-angle (greater *d* spacing) reflection. These two factors suggest the coexistence of two discrete hydration states during a change from two to three water layers and is consistent with previous studies into the Al-rich, dioctahedral smectite, beidellite (Suquet *et al.*, 1975). The original 001 reflection for all samples occurred at ~15 Å while the hydrated state was at ~19.5 Å. Note that the ratio of intensities between the 001 reflection and the diffraction peak at 4.5 Å was less for NAu-2 than for NAu-1 and Nont2g in either the 'as received' or hydrated state. Note also that the diffraction peak apparent at ~4.5 Å is actually the product of several overlapping reflections at $\bar{1}10$, 020, and $1\bar{1}\bar{1}$ (Bayliss, 1989). Heating of the hydrated clays to 125ºC with appropriate hydrothermal pressure produced a decrease in *d* spacing for all samples. NAu-1 is the 'purest' nontronite and had the greatest reduction in *d* spacing with a shift from ~19.5 Å to ~16.7 Å. The integrated intensity of this peak remained reasonably constant throughout the duration of the reaction but a loss of crystallinity or the coexistence of a range of compositions was indicated by its broadening. The broadening may indicate a removal of some interlamellar H_2O with temperature, resulting in interstratification of different hydration states due to the more random distribution of water layers. NAu-2 moved

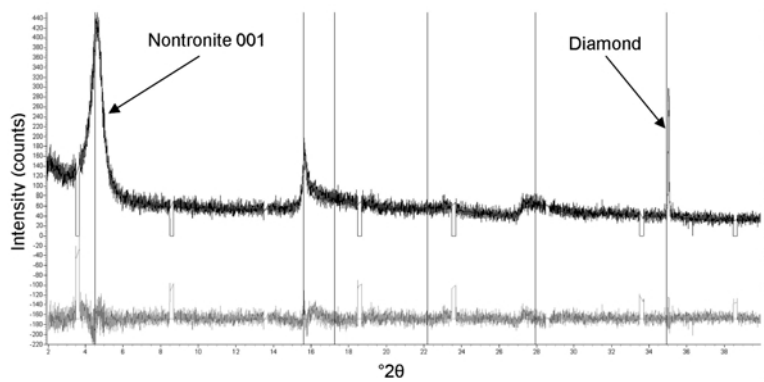

Figure 3. Fitted diffraction pattern (black) of NAu-1 showing peak positions (vertical lines), calculated pattern (mid-grey), and difference curve (light-gray). Note the excluded regions in the calculated pattern at the intersections of the detector segments.

https://doi.org/10.1346/CCMN.2011.0590602 Published online by Cambridge University Press

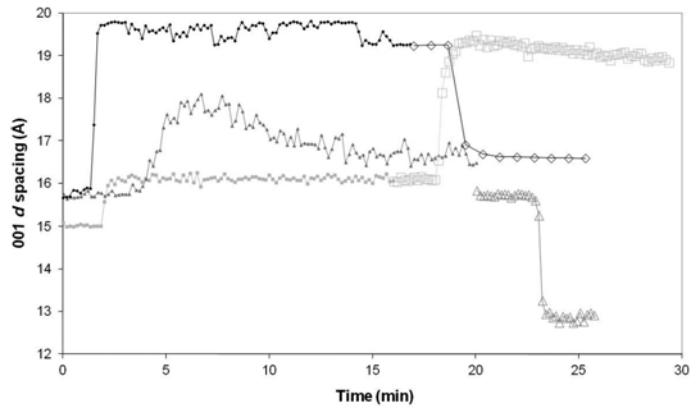

Figure 4. Movement of the 001 reflection of NAu-1 on reaction with: (1) H_2O (black diamonds), (2) low acid solution (light gray squares), and (3) high acid solution (mid-gray triangles) at room temperature (solution injection: small, solid symbols) and 125ºC (slurry: large, open symbols). (Note only every fifth data point has been plotted for clarity.)

from ~19.7 Å to ~19.2 Å and Nont2g moved from ~19.9 Å to ~19.0 Å. Nont2g was similar to NAu-1 in that the 001 reflection in the hydrated state broadened with time; however, in this case the broadening was asymmetric with the low-angle side increasing preferentially. This too may indicate the coexistence of different hydration states.

Acid attack on smectites is traditionally believed to occur *via* removal of the exchangeable cations from the interlayers followed by removal of the octahedral cations and those substituting for Si in the tetrahedral sheet (Madejová *et al.*, 1998). However, the behavior observed during simulated high-pressure acid leaching of the nontronites considered in the present study is more complex than this mechanism suggests. Replacement of the interlayer cations with H^+ (actually present in hydrated form, H_3O^+) from the acid or Fe^{3+} or Al^{3+} from the layers should cause a contraction in the interlayer distance due to the smaller ionic radii of these species compared with typical exchangeable cations (Ca^{2+}, Na^+). The results presented here indicate possible competing mechanisms combining the effects of hydration and acid attack.

The introduction of the low acid caused an initial expansion in all the samples considered, probably through hydration. The 001 reflection of NAu-1 moved from ~15 Å to ~16 Å with asymmetric broadening (low-angle side larger). The broadening may actually be the formation of lower-angle peaks (overlapping) which coexist with the original peak and are indicative of interstratification. On heating to 125ºC, two distinct peaks appeared with the lower-angle peak (~19 Å) increasing in intensity at the expense of the higher-angle reflection. This may represent the transformation of the clay from one hydration state to another with the interstratified coexistence of the two structures prior to the expansion of the cell on heating.

Low acid caused the movement of the 001 reflection of NAu-2 from ~15 Å to ~16.3 Å and Nont2g from ~15.1 Å to ~16.8 Å. However, the application of heat (125ºC) caused considerable further expansion in NAu-1 (to 19.5 Å) and Nont2g (to ~20 Å) but collapse (to

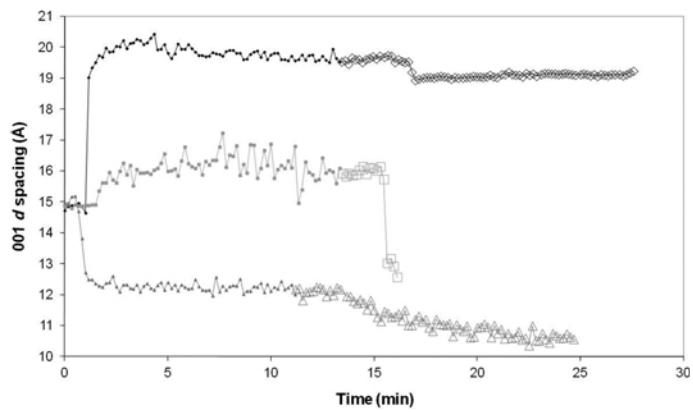

Figure 5. Movement of the 001 reflection of NAu-2 on reaction with: (1) H_2O (black diamonds), (2) low acid solution (light gray squares), and (3) high acid solution (mid-gray triangles) at room temperature (solution injection: small, solid symbols) and 125ºC (slurry: large, open symbols). (Note only every fifth data point has been plotted for clarity.)

https://doi.org/10.1346/CCMN.2011.0590602 Published online by Cambridge University Press

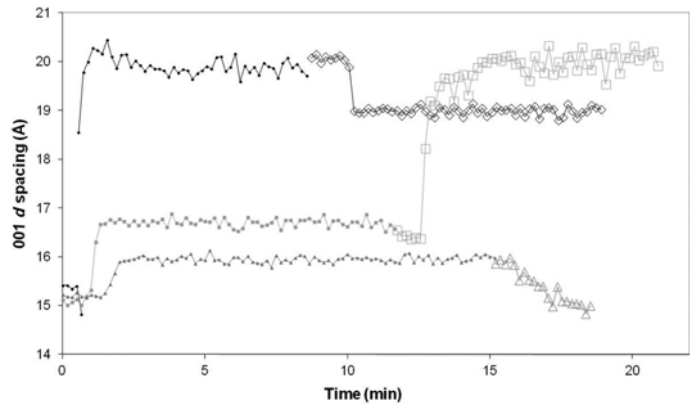

Figure 6. Movement of the 001 reflection of Nont2g on reaction with: (1) H_2O (black diamonds), (2) low acid solution (light gray squares), and (3) high acid solution (mid-gray triangles) at room temperature (solution injection: small, solid symbols) and 125ºC (slurry: large, open symbols). (Note only every fifth data point has been plotted for clarity.)

~12.4 Å) and dissolution in NAu-2. NAu-1 appeared to contract slightly over the next 10 min of reaction time but Nont2g remained stable in its expanded state. NAu-2 also behaved differently to the other two in the presence of high acid. NAu-1 experienced an initial expansion (from ~15.7 Å to ~17.9 Å) followed by a gradual contraction while still at room temperature as acid attack began to replace interlayer cations with H^+. The acid subsequently attacked the layers and began to remove Al^{3+} and Fe^{3+} which are thought to also report initially to the interlayer regions. The application of heat caused a rapid contraction of the clay (to ~12.8 Å) as it lost crystallinity while the structure collapsed, with the increased dissolution of Al^{3+} and Fe^{3+} from the layers also resulting in lower layer charge and the formation of amorphous silica. Nont2g underwent a small expansion (from ~15.1 Å to ~15.9 Å) on the introduction of high acid, which appeared stable over a period of some minutes. Heating produced rapid dissolution with an initial contraction shown by movement of the 001 reflection to ~15 Å. Once again NAu-2 differed from the other two clays in that it contracted immediately to ~12.3 Å upon addition of high acid. This condition seemed stable until the application of heat which caused further gradual contraction (to ~10.2 Å during the time of the experiment) and loss of crystallinity.

Dehydration

NAu-1 and NAu-2 were also heated to 300ºC in capillaries in air at a rate of 20ºC/min to assess their dehydration behavior. Datasets of 10 s duration were collected continuously throughout heating. Accumulated stacks of synchrotron XRD patterns from the experiments for NAu-1 (Figure 7) and NAu-2 (Figure 8) revealed patterns similar in form to those shown in Figure 2, but in this case the data are viewed down the intensity axis. The temperatures corresponding with the data-set numbers on the vertical axis have been superimposed on the figures.

The d_{001} of NAu-1 contracts from ~15 to 9.5 Å over the entire period of temperature increase (~13.5 min) corresponding to the shift in diffraction angle from ~5 to 7.25º2θ (Figure 7). The reflection began to broaden around 150ºC, reached a maximum at 250ºC, and sharpened gradually up to 300ºC. Slight continued sharpening was apparent with time at 300ºC. The peak broadening was consistent with that observed in the hydration experiment (see the 'Hydration and leaching' section), indicating a tendency for this mineral to interstratify with different hydration states, meaning that the broadened peak contains the 001 reflections

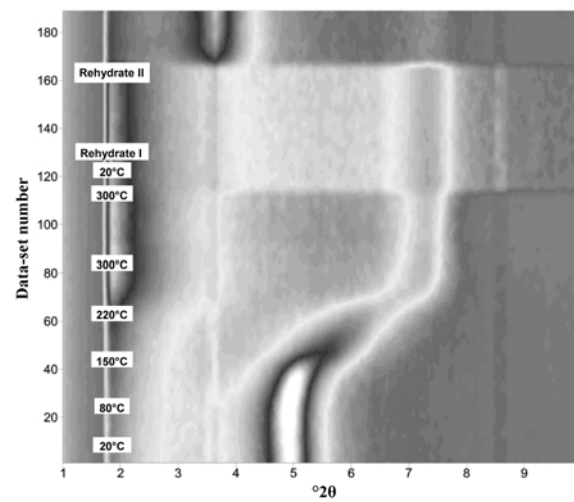

Figure 7. Accumulated synchrotron XRD patterns from the dehydration of NAu-1 in air. The data are represented as a three-dimensional plot viewed down the intensity (z) axis with diffraction angle along the x axis and data-set number along the y axis. The 001 reflection of nontronite can be seen to move to a higher diffraction angle (lower d spacing) with dehydration. 'Rehydrate I' represents the first attempt to rehydrate the material, which was unsuccessful; 'Rehydrate II' represents the second, successful attempt.

https://doi.org/10.1346/CCMN.2011.0590602 Published online by Cambridge University Press

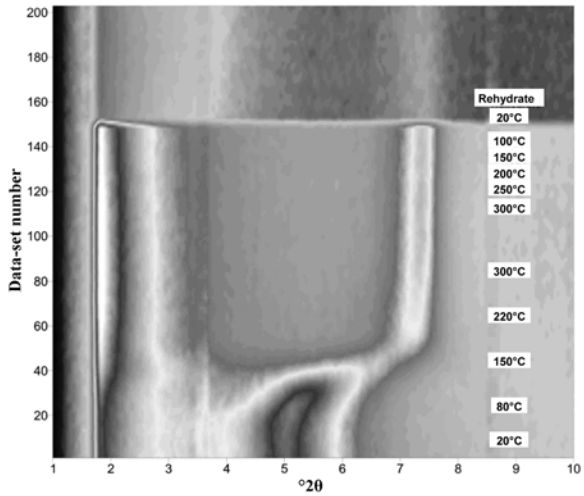

Figure 8. Accumulated synchrotron XRD patterns from the dehydration of NAu-2 in air. The data are represented as described in Figure 7. 'Rehydrate' indicates the point at which data collection was recommenced following rehydration.

from a number of hydration states. Rehydration of the sample produced a considerable reduction in the area of the ~9.5 Å (7.25º2θ) peak and the appearance of a second reflection with d_{001} of ~19.5 Å (~3.5º2θ), indicating incomplete rehydration and the coexistence of hydrated and dehydrated species. Note that the initial moment of rehydration was not recorded in the data as it was carried out manually with the X-ray shutter closed.

The d_{001} of NAu-2 contracted with a similar shift of reflection to NAu-1 (~2.25º2θ) over the entire range of temperature increase. The reflection began to broaden (increased peak area) at ~120ºC, reached a maximum at ~150ºC, and sharpened gradually up to ~200ºC. During this broadening the shape became asymmetric and changed the center of its asymmetry from low to high angle (Figure 9). This is suggestive of two components dehydrating at different temperatures. Little further peak sharpening was apparent between 200 and 300ºC. Rehydration of the sample resulted in its almost complete loss of crystallinity (Figure 10). The inability to rehydrate may be related to the balance of the layer charge in this mineral. Calculation of structural formulae (Gates *et al.*, 2002) showed that the ratio of tetrahedral to octahedral negative charges per unit cell of NAu-1 and NAu-2 were 1.02 (T) to 0.03 (O) and 0.45 (T) to 0.26 (O), respectively. The greater negative charge in the octahedral sheet of NAu-2 may have impinged upon its ability to rehydrate, although the tetrahedral charge of this nontronite was too high for truly montmorillonite-like behavior.

Following this finding of different behavior between the two standard nontronites, an *in situ* dehydration of Nont2g was undertaken in the laboratory using the Inel diffractometer incorporating the CPS120 position-sensitive detector, capable of the simultaneous detection of 120º2θ of the diffraction pattern. The diffractometer was fitted with a Co long fine-focus tube operated at 35 kV and 30 mA. The incident beam was defined using a curved multilayer mirror to pass only the $K\alpha_{1,2}$ wavelengths and 0.3 by 8.0 mm vertical and horizontal slits, respectively. This nontronite showed a similar magnitude of contraction of d_{001} to the others but the peak broadening, which commenced at lower temperature (~80ºC), reached a maximum at ~120ºC and sharpened gradually with continued heating. Similarly to NAu-2, attempted rehydration of the sample resulted

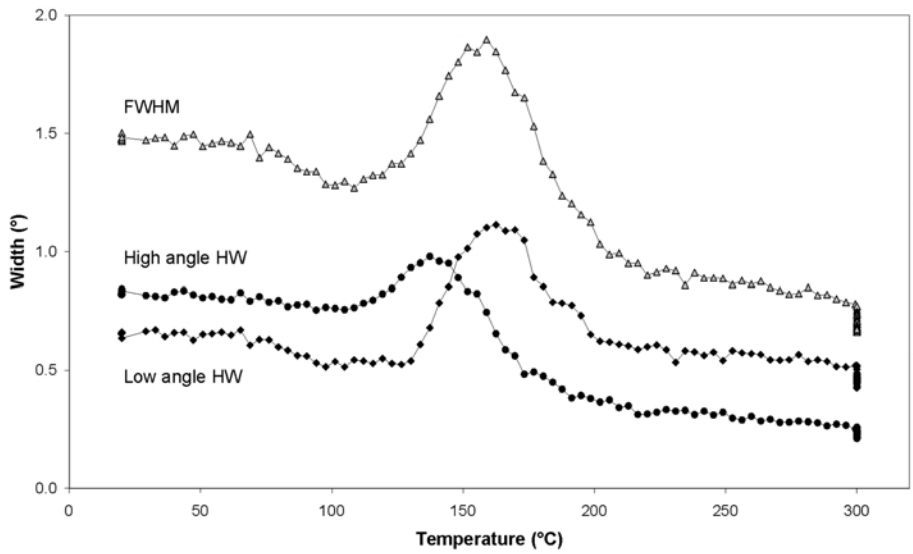

Figure 9. Refined peak-width parameters for the dehydration of NAu-2 in air. The parameters are from the split pseudo-Voigt model used to model the peak.

https://doi.org/10.1346/CCMN.2011.0590602 Published online by Cambridge University Press

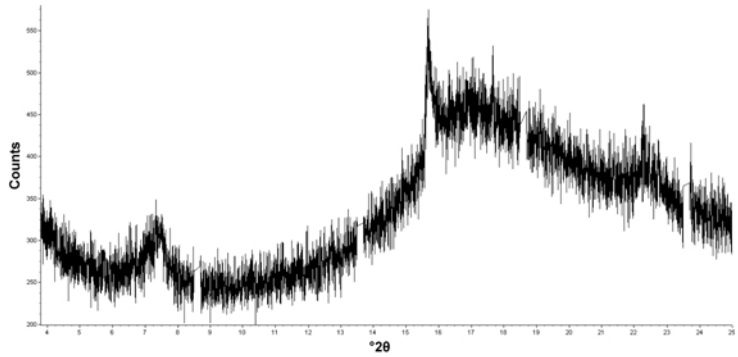

Figure 10. Diffraction pattern of NAu-2 following the attempt to rehydrate it after dehydration at 300ºC. The gaps in the data result from the gaps between the modules in the Mythen detector.

in its almost complete loss of crystallinity (*i.e.* long-range order).

The changes in the d_{001} of NAu-1, NAu-2, and Nont2g with dehydration may be compared as a function of temperature (Figure 11). NAu-1 appeared to lose its water mainly in two steps at ~160ºC and ~240ºC with gradual change in between, suggesting interstratification of different hydration states throughout the process. NAu-2 also lost water in two steps but the initial loss was more gradual beginning at ~60ºC, followed by a distinct increase in rate from ~130ºC and finishing by ~170ºC. Nont2g also appeared to dehydrate in two steps: one at ~80ºC and one ~120ºC, with dehydration complete by ~170ºC. These temperatures also corresponded to the peak broadening described above. The diffraction patterns of each of the clays at room temperature, heated, and following rehydration were plotted and compared directly (Figure 12). The similarity in contraction of d_{001} on dehydration was clear in all specimens, while higher-angle reflections were unaffected. The disappearance of d_{001} in NAu-2 and Nont2g on rehydration was also apparent whereas in NAu-1 this reflection reappeared at a higher d spacing. In all samples a small peak remained at the position of the dehydrated d_{001} reflection, suggesting incomplete rehydration in all cases.

CONCLUSIONS

The effects of hydration, acid attack, and dehydration on three different nontronite samples were studied using powder XRD. In all three samples studied, the addition of water led to the coexistence of discrete hydration states. Heating of these hydrated samples then caused a rearrangement of the interlamellar water and asymmetric broadening of the 001 reflection consistent with interstratification of different hydration states. The Source Clays, NAu-1 and NAu-2, appeared to dehydrate *via* slightly different mechanisms at slightly different temperatures. Attempts to rehydrate the fully dehydrated NAu-2 resulted in a loss of crystallinity. In contrast, the addition of water to dehydrated NAu-1 produced a material the XRD pattern of which was consistent with incomplete rehydration and the coexistence of hydrated and dehydrated species. The major difference between these samples was the source of the layer charge. NAu-2 has layer charge distributed over both tetrahedral and octahedral sheets in contrast to NAu-1 which has the

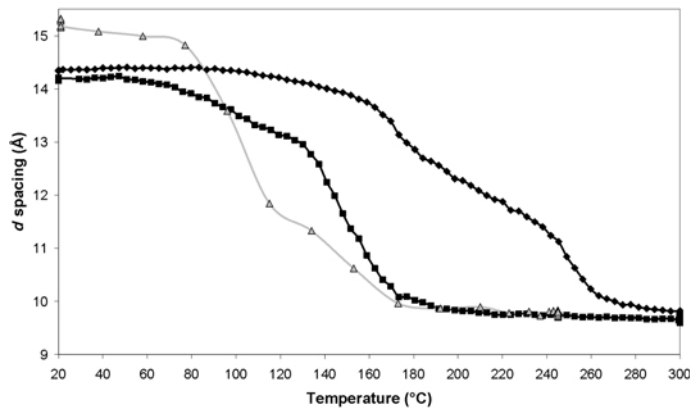

Figure 11. Comparison of the movement of the 001 reflection of NAu-1 (black diamonds), NAu-2 (mid-gray squares), and Nont2g (light gray triangles) with heating in air.

https://doi.org/10.1346/CCMN.2011.0590602 Published online by Cambridge University Press

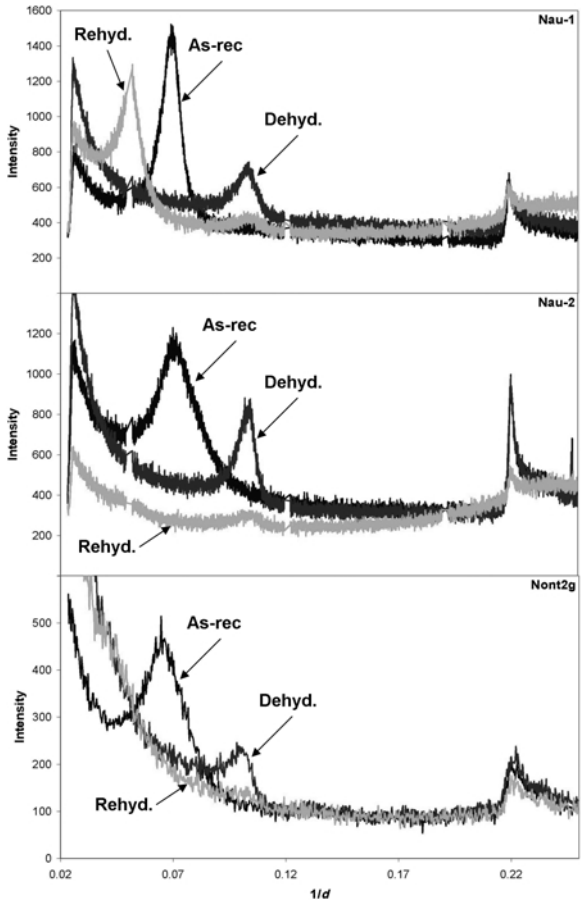

Figure 12. Comparison of the diffraction patterns of NAu-1, NAu-2, and Nont2g as received (As-rec), at 300ºC (Dehyd.), and following rehydration (Rehyd.). The gaps in the data from NAu-1 and NAu-2 result from the gaps between the modules in the Mythen detector.

source of the layer charge predominantly in the tetrahedral sheet. This may contribute to the different response to dehydration and rehydration of these materials.

High-pressure acid leaching of these samples produced results indicative of competing mechanisms of hydration and acid attack, the nature of which also appears related to the structural formula of the clay. NAu-2 appeared to be more susceptible to acid attack than NAu-1 which may be a function of the presence of Fe(III) in its tetrahedral sheet. Acid has been shown to remove tetrahedral and octahedral Fe(III) from nontronite at similar rates (Komadel and Madejová, 2006; Luca and MacLachlan, 1992) and, therefore, may contribute to the ready dissolution of NAu-2. NAu-1 has a larger cation exchange capacity because of its greater layer charge which may delay acid attack on its sheets.

Nont2g behaved similarly to NAu-2 in terms of its inability to rehydrate whilst its response to high-pressure acid leaching was more akin to that of NAu-1. No determination of the charge distribution of Nont2g was carried out so further examination of the reasons for this behavior was not possible.

ACKNOWLEDGMENTS

The authors acknowledge: Nicki Agron-Olshina, Matthew Rowles, Sally Taylor, and Nathan Webster for assistance with data collection; support for beamtime from the Australian Synchrotron under grant number 102_AS07/3011; and the assistance of the beamline scientist Kia Wallwork.

REFERENCES

Bayliss, P. (1989) Unit-cell determinations of two-dimensional clay minerals. *Powder Diffraction*, **4**, 19–20.

Bruker AXS. (1999) *Topas v3*: General profile and structure analysis software for powder diffraction data.

Dalvi, A.D., Bacon, W.G., and Osborne, R.C. (2004) The past and the future of nickel laterites. *PDAC 2004 International Convention, Trade Show & Investors Exchange*.

Gates, W.P., Slade, P.G., Manceau, A., and Lanson, B. (2002) Site occupancies by iron in nontronites. *Clays and Clay Minerals*, **50**, 223–239.

Keeling, J.L., Raven, M.D., and Gates, W.P. (2000) Geology and characterisation of two hydrothermal nontronites from weathered metamorphic rocks at the Uley graphite mine, South Australia. *Clays and Clay Minerals*, **48**, 537–548.

Komadel, P. and Madejová, J. (2006) Acid activation of clay minerals. Pp. 263–287 in: *Handbook of Clay Science* (F. Bergaya, B.K.G. Theng, and G. Lagaly, editors). Elsevier Ltd., Amsterdam.

Madejová, J., Bujdak, J., Janek, M., and Komadel, P. (1998) Comparative FT-IR study of structural modifications during acid treatment of dioctahedral smectites and hectorite. *Spectrochimica Acta Part A*, **54**, 1397–1406.

Madsen, I.C., Scarlett, N.V.Y., and Whittington, B.I. (2005) Pressure acid leaching of nickel laterite ores: An in situ diffraction study of the mechanism and rate of reaction. *Journal of Applied Crystallography*, **38**, 927–933.

Norby, P., Cahill, C., Koleda, C., and Parise, J. B. (1998) A reaction cell for in situ studies of hydrothermal titration. *Journal of Applied Crystallography*, **31**, 481–483.

Scarlett, N.V.Y., Madsen, I.C., and Whittington, B.I. (2008) Time-resolved diffraction studies into the pressure acid leaching of nickel laterite ores: A comparison of laboratory and synchrotron X-ray experiments. *Journal of Applied Crystallography*, **41**, 572–583.

Schmitt, B., Brönnimann, C., Eikenberry, E.F., Gozzo, F., Hörmann, C., Horisberger, R., and Patterson, B. (2003) Mythen detector system. *Nuclear Instruments and Methods in Physics Research Section A*, **501**, 267–272.

Suquet, H., de la Calle, C., and Pezerat, H. (1975) Swelling and structural organisation of saponite. *Clays and Clay Minerals*, **23**, 1–9.

Whittington, B.I., McDonald, R.G., Johnson, J.A., and Muir, D. (2003) Pressure acid leaching of arid-region nickel laterite ore: Part I: Effect of water quality. *Hydrometallurgy*, **70**, 31–46.

(*Received 17 June 2009; revised 24 August 2011; Ms. 327; A.E. J.D. Fabris*)